Construction and Building Materials 404 (2023) 133189

Contents lists available at ScienceDirect

Construction and Building Materials

journal homepage: www.elsevier.com/locate/conbuildmat

Parametric analysis in sustainable self-compacting mortars using genetic programming

Gemma Rojo-López, Belén González-Fonteboa *, Juan Luis Pérez-Ordóñez, Fernando Martínez-Abella

Universidade da Coruña (UDC), Civil Engineering School, Centro de Innovación Tecnolóxica en Edificación e Enxeñaría Civil (CITEEC), Campus Elviña s/n, La Coruña 15071, Spain

ARTICLE INFO

Keywords:
Genetic programming
Supplementary cementitious materials
Biomass ash
Granite powder

ABSTRACT

This study addresses the capabilities of genetic programming to predict the behaviour of cement-based mixtures by focusing on the influence of quaternary binders (incorporating metakaolin, biomass ash and granite powder as novel powder materials) on the rheological properties of self-compacting mixtures, including spread diameter in mini-cone test and time to flow in mini-funnel test. Using a previous dataset, GP techniques are applied to obtain predicted models and to compare them with those developed throughout analysis of variance. The results demonstrate that the equations obtained by the GP technique showed the best statistical indices for the analysed properties. Afterwards, a parametric analysis was performed to analyse the influence of the composition of quaternary binders on the fresh behaviour of mortar mixtures. The parametric analysis indicated that changes in the binder composition that increased granite powder content damage the fresh behaviour of the mortars (the funnel time increases, and the spread diameter decreases), being this negative effect more significant when the water content is low, and especially noteworthy in the Tfunnel time. It is concluded that genetic programming and design of experiments are powerful tools that can be used to analyse the influence of new raw materials in different mortar properties.

1. Introduction and objectives

The cement production industry, and consequently the building industry, contributes a significant percentage of the greenhouse gases emitted into the atmosphere [1–3]. Moreover, the requirement for cement is not likely to decrease in the short term as cement demand is forecast to reach 6 billion tonnes per year by 2060 [4]. Alternative materials are therefore essential to partially replace cement, thus contributing to the development of more sustainable and environmentally friendly materials. This is the case of sup. lementary cementitious materials (SCMs), such as silica fume (SF), fly ash (FA), and ground granulated blast-furnace slag (GGBS), which are widely used. There is therefore wide information on both their fresh [5,6] and hardened performance [7–9]. Rojo et al. [10] assessed the effect of the solid volume fraction on both concrete rheology for binary and ternary mixtures by replacing cement with metakaolin (MK) and limestone filler (LF) at four paste volumes. Solomon et al. [11] analysed the behaviour of FA, SF and MK at high temperatures to construct by using fire-resistant concrete, thus improving occupant safety in the event of a fire. AL-Radi et al [12] also carried out high temperature studies on self-compacting concretes containing SF, including in the analysis the reinforcement of both metallic and polypropylene fibres. However, it is important to explore new opportunities derived from industrial waste that can provide new routes towards a more sustainable building industry [13,14].

To select these by-products, a wide knowledge about the material and an extensive experimental campaign are required to test their suitability, effects and interactions in mixtures in both the short and the long term. This is time-consuming and resource-consuming. Jhatial et al. [15] reviewed several emerging cementitious materials and concluded that the lack of studies on the effects of incorporating SCMs in concrete in the short and long term is one of the reasons why SCMs are not used at an industrial scale. Therefore, further research studies on mechanical and durability properties are required to propose the implementation of these emerging SCMs in industrial applications.

* Corresponding author.
E-mail addresses: gemma.rojo@udc.es (G. Rojo-López), bfonteboa@udc.es (B. González-Fonteboa), juan.luis.perez@udc.es (J. Luis Pérez-Ordóñez), fmartinez@udc.es (F. Martínez-Abella).

https://doi.org/10.1016/j.conbuildmat.2023.133189
Received 12 May 2023; Received in revised form 28 August 2023; Accepted 29 August 2023
Available online 6 September 2023

Knowledge extraction techniques can be used in construction industry research to reduce time and resource consumption of extensive experimental campaigns. These techniques can range from simple linear regression models to sophisticated machine learning (ML) techniques. All these methods have their benefits and drawbacks, e.g. regression models are simple [16], but a large database is necessary to ensure that the confidence of the models is not reduced, so many experimental results are required. As for ML, different techniques with their advantages and disadvantages can be used.

For example, the artificial neural network (ANN) is a common method to assess the mechanical properties of concrete to obtain a predictive model [3,4], but the model works as a black box, i.e. solutions are obtained, but it is not easy to obtain the model in a mathematical expression.

Another ML method that effectively designs and solves non-linear regression problems is the support vector machine (SVM). This method has shown strong generalization abilities and is useful to obtain better global optimum results [16,17]. The response parameter can also be predicted using tree-like structures by using ensemble learning techniques, such as decision tree (DT) and random forest (RF) techniques. While RF randomly selects the important parameters and builds multiple ensemble learning trees for predictions, DT uses the entire dataset with the variables of interest. An accurate estimate is then obtained by estimating the averaged values of these forecasts and by setting the result with the majority of votes [18]. Both SVM and RF techniques do not provide a straightforward mathematical equation, so they are used only as predictors. Researchers therefore forecast more accurate outcomes by using the SVM and RF algorithms' robust structural designs.

Likewise, they are increasingly used in different fields. In the field of civil engineering and building, using methods that provide mathematical equations as a result is essential. For this reason, the genetic programming (GP) technique is excellent because it provides a prediction equation to use in the future on unobserved data. This means that these equations can be used for the design of different mixtures or for parameter settings without needing the knowledge associated with the application of machine learning techniques [19]. In fact, Ma et al. [20] in their study of a backbone curve model of reinforced concrete walls show that the use of GP provides explicit equations that are easily interpretable and easy to use by researchers and engineers. Likewise, the GP method provides a mathematical equation to obtain an accurate result, thus modelling complex applications in civil engineering in recent years [1,20–22].

In the literature, various ML techniques have been used in the field of civil engineering. Many of them are used to analyse the concrete hardened state [23]. However, with the increasing development of new concretes where rheology plays a fundamental role, the employment of these techniques in the field of the fresh state has also grown [23–28]. Nazar et at. [23] analyse the concrete fresh properties with a database obtained from previous studies via decision tree and bagging regressor. The same authors predict explicit equations for yield stress and plastic viscosity [27]. In both these works, the influence of some mixing parameters (cement content, water content, sand…) was analysed, being, however, the cement type the same in all mixes. Aziminezhad et al. [26] analyses the rheological properties for ternary binders using response surface method (RSM) to assess the influence of water to cement ratio and superplasticiser dosage when salg and silica fume are added to the mixtures. Other works [24,25] analyse the presence of blended cements (with fly ash, silica fume, and nanoclay) and how the variation in the design parameters affect the fresh properties. In these works, however, there is no explicit equation that can be used to compare the results.

This work belongs to a wide research campaign that aims to achieve the integral design of sustainable concretes. Within this goal, in this work, it was decided to act on concrete mix design introducing the use of recycled sup. lementary cementitious materials replacing clinker and improving the efficiency of different aspects of the production process (cost reduction, shortening of construction timeframes or safety improvements). The combination of these aspects led to the design of sustainable self-compacting concretes with blended cements.

Furthermore, properly designed and placed self-compacting concrete will show similar properties regarding its hardened state and durability as its homologue vibrated concrete but will differ in its behaviour in fresh state. Therefore, the main objective of this work is the study and prediction of the fresh state behaviour of sustainable self-compacting concretes introducing sup. lementary cementitious materials in their mix design.

In fresh behaviour concrete can be considered as a suspension where the mortar is the solution, and the coarse aggregates are the suspended particles. In this work, mixes have been designed so that the solid volume fraction (the coarse aggregate) does not vary with the aim of analysing the influence of the different sup. lementary cementitious materials used to replace clinker. In this situation, the fresh behaviour of the concretes is going to be controlled by the mortar phase, that is why the study is focused on analysing the fresh behaviour of self-compacting mortars.

The main objective of this work is then the assessment of the influence of various quaternary binders in the fresh state of self-compacting mortars. The binders designed in this study are composed of cement and three novel SCMs (metakaolin, biomass ash and granite powder) that have not been widely used as fillers, which justifies the novelty of analysing their effect on the mortar fresh properties using different tools. In a previous work a dataset was developed and regression analysis using ANOVA was employed [29]. In this work, using the same dataset, to better analyse and to predict the influence of the novel sup. lementary cementitious materials in the fresh behaviour of the mortar mixes it was decided to employ genetic programming technique and compare the results with the previous analysis. This technique, on opposition to other tools as ANN, has the advantage of providing with explicit equations where the influence of the main variables affecting the fresh properties can be assessed. These equations can be easily used by the stakeholders, which, undoubtedly will promote the employment of the new concretes in the construction field.

The properties studied are as follows: spread diameter in mini-cone test and flow time in mini-funnel test. As for mini-cone and mini-funnel results, the objective was both to apply GP techniques to the dataset and to compare the models obtained with the regression analysis [29]. For this purpose, statistical parameters were studied to obtain models that improve the predictions. Moreover, a parametric analysis was carried out to understand how the different parameters controlling the content of the novel sup. lementary cementitious materials affect the fresh state properties of the mortars.

2. Materials and mixes

Four powder materials were used: Portland cement labelled as CEM I 52.5 N-SR5 (CEM), biomass ash (BA), granite powder (GP), and metakaolin (MK) as SCMs. Cement and MK are standard commercial materials from Spanish companies. The BA and GP are wastes that were collected directly from the manufacturing plants where they are produced, a timber board manufacturing plant in the case of BA and a granite quarry in the case of GP (both situated in Spain). Fig. 1 includes images of these materials under the scanning electron microscope (SEM).

Their physical and chemical properties are included in Table 1, and the particle size distribution (PSD) is shown in Fig. 2. MK is a pozzolanic material [30] that can be widely used to partially replace cement. GP is an industrial waste material obtained by cutting granite rocks, and the BA used in this work is also an industrial waste obtained from wood industry [29].

Table 1 includes the chemical composition obtained by the X-Ray-Fluorescence technique and the specific density by helium pycnometry. The particle density (N_{PSD}) calculated by using the PDS model described

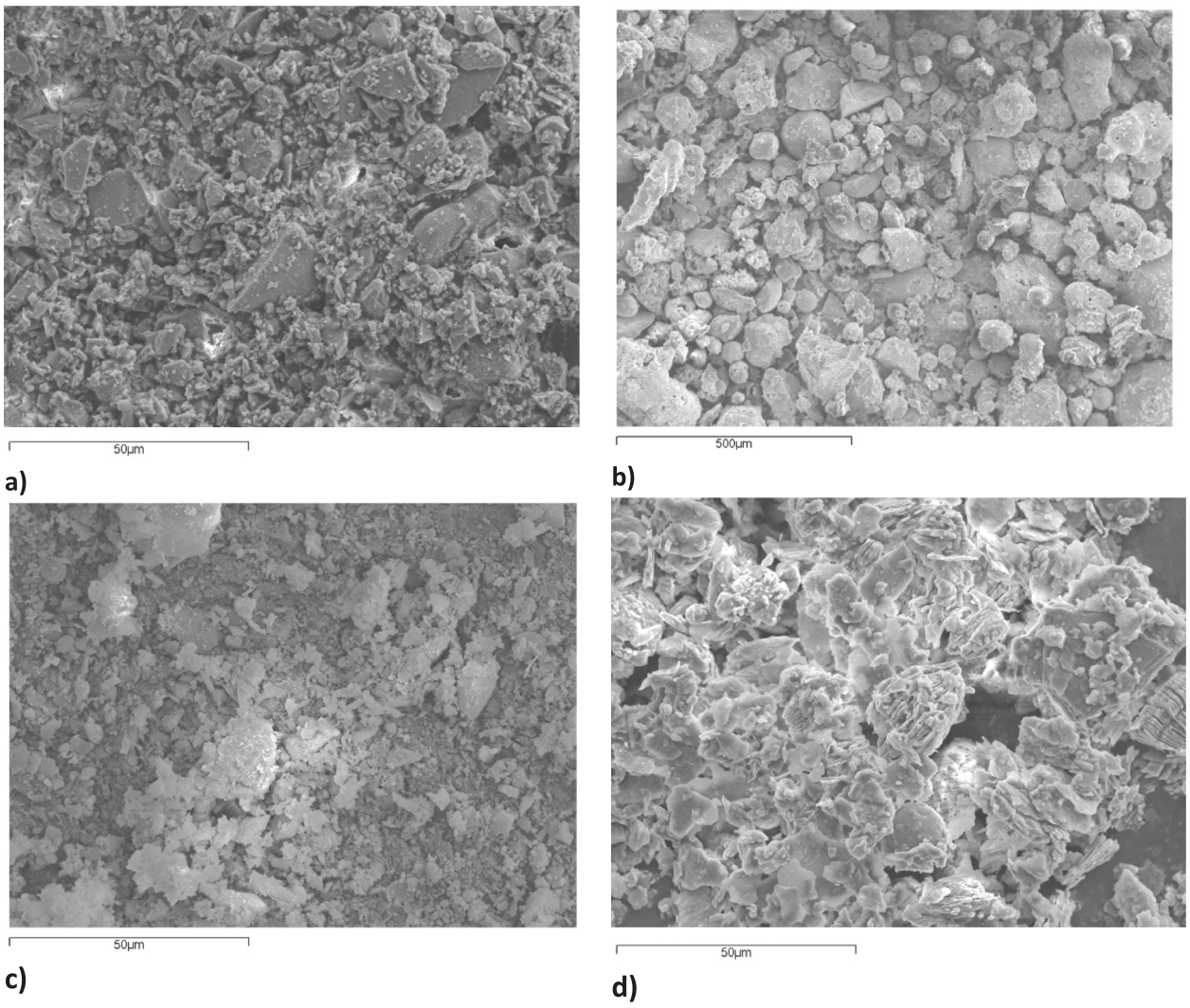

Fig. 1. SEM images: a) CEM. b) BA. c) GP. d) MK.

Table 1
Physical and chemical properties of powder materials.

% by mass	CEM	BA	GP	MK
SiO_2	18.9	40.0	70.4	58.0
Al_2O_3	6.3	16.6	15.2	36.8
Fe_2O_3	2.7	5.5	2.0	1.2
CaO	59.9	10.2	1.0	0.075
K_2O	1.9	6.9	5.5	2.1
Na_2O		1.6	3.7	
MgO	1.6	2.8	0.35	0.18
SO_3	3.5	2.4		0.058
LOI	4.3	2.7	1.0	0.7
Specific density (g/cm^3)	3.04	2.68	2.77	2.55
Particle density – N_{PSD} [31]	23	19	40	1
Packing density [32]	0.48	0.45	0.39	0.30
Pozzolanic activity (mg of $Ca(OH)_2$)[33]		946	48	946

in the literature [31], so it was assumed that particles are spherical in shape.

The values of the dry packing density measured using the method described by Wong et al. [32] are also included. Both properties were used to understand the fresh behaviour of mixtures. Finally, the pozzolanic activity was determined by modified Chappelle test according to French standard NF P18-513 [33].

Fig. 2 includes the gradation of all the powder materials measured by laser diffraction. Moreover, cement and MK showed a similar fineness, while GP and BA were finer and coarser, respectively, than the cement.

To control workability, tap water and a polycarboxylate-based superplasticizer were used in the mix design. Finally, a standard sand was used in the mortar mixtures according to EN 196-1 [34].

Mortar mixtures came from a previous study in which the experimental programme has been defined according to a Central Composite Design plan with a complete 2^4 factorial plan, corresponding to four factors and two levels per factor. Furthermore, taking into account that the investigated properties were not expected to change linearly within the experimental region, axial points (CCi) and centre points (Ci) were added to the factorial plan [35]. The following independent variables were selected: water to powder volume ratio (V_W/V_P), water to cement weight ratio (w/c), superplasticizer to powder weight ratio (Sp/p), and BA to cement weight ratio (ash/c). The effects of these variables were evaluated at five different levels by defining the range of variation shown in Table 2. Further details on the selection of these ranges can be found in [29,35]. Fine aggregate content was constant (1249.25 kg/m^3), leading to a sand to mortar volume ratio (Vs/Vm) of 0.475. In addition, a fixed MK to cement weight ratio was defined (MK/c = 0.20). According to these parameters, 25 different mortar mixtures were designed (Table 3).

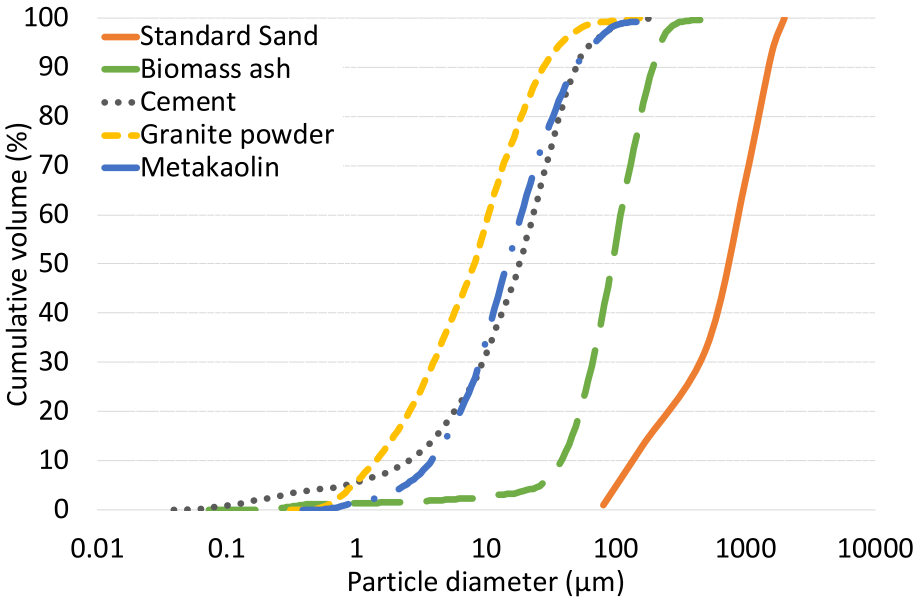

Fig. 2. Grading curves of the powder materials.

Table 2
Range of the independent variables used in the mortar mix design.

Independent variables	−2	−1	0	−1	−2
V_W/V_P	0.75	0.8	0.85	0.9	0.95
w/c	0.4	0.45	0.50	0.55	0.6
Sp/p	0.015	0.0155	0.016	0.0165	0.017
ash/c	0.1	0.15	0.15	0.175	0.2

Table 3
Mortar mixes (kg/m^3).

Ref	CEM	MK	BA	GP	Sp	Water
Ci (i = 1–6)	480.57	96.11	26.88	59.83	13.03	240.29
F1	516.52	103.30	24.07	55.83	13.00	232.44
F2	550.61	110.12	25.66	25.10	12.38	247.77
F3	422.62	84.52	19.70	98.51	12.90	232.44
F4	450.51	90.10	21.00	70.59	12.28	247.78
F5	516.40	103.28	24.07	55.81	13.84	232.38
F6	550.48	110.10	25.66	25.09	13.18	247.71
F7	422.52	84.50	19.69	98.48	13.73	232.39
F8	450.40	90.08	20.99	70.57	13.07	247.72
F9	516.53	103.31	33.70	46.20	12.99	232.44
F10	550.61	110.12	35.93	14.83	12.37	247.77
F11	422.62	84.52	27.58	90.63	12.89	232.44
F12	450.51	90.10	29.40	62.19	12.27	247.78
F13	516.40	103.28	33.69	46.19	13.82	232.38
F14	550.48	110.10	35.92	14.83	13.17	247.72
F15	422.52	84.50	27.57	90.60	13.72	232.39
F16	450.41	90.08	29.39	62.18	13.06	247.72
CC1	448.17	89.63	25.07	90.95	13.71	224.09
CC2	509.66	101.93	28.50	31.89	12.42	254.83
CC3	600.69	120.14	33.60	4.11	13.16	240.28
CC4	400.49	80.10	22.40	96.97	12.94	240.29
CC5	480.69	96.14	26.88	59.84	12.22	240.34
CC6	480.46	96.09	26.87	59.81	13.84	240.23
CC7	480.57	96.11	17.92	68.79	13.04	240.29
CC8	480.57	96.11	35.84	50.87	13.02	240.29

3. Testing protocols

According to EN 196E1, all mortar mixtures were produced in 1.6 l batches and mixed in a mixer at a low constant speed (140±5 rpm), following the mixing procedure described in Fig. 3. Fig. 4.

The powder materials and 80% of mixing water were mixed for one minute at a low constant speed (140±5 rpm). The mixer was stopped for a short time to remove the material adhered to the walls of the container, and then the rotation was started for another minute. At the end of this period, the superplasticiser and the remaining water were added. The mixing continued for another 2 min, the mortar was left to rest for 2 min, and finally it was mixed again for an additional period of 2 min using, in this case, a high speed (285±10 rpm). More information about the mixing protocol can be seen in a previous paper [29].

Afterwards, a wide experimental campaign was conducted to measure the fresh and hardened state of mortars. However, only the results from mini-slump (Dflow-mm) and mini-funnel (Tfunnel-s) were used. Both tests were performed just after the mixing. The value used in this study was the average of both measurements.

4. Genetic programming (GP)

The results of the rheological behaviour obtained in the experimental programme were analysed using the GP technique. It consisted of a subset of solution search techniques based on evolutionary computation. An analogy was therefore established between the set of solutions to a given problem and the set of individuals in a natural population that adapted to the environment (problem) and similarly to biology natural selection. The solution to the problem was the best-adapted individual. The information of each solution was encoded by means of a tree structure. Two types of nodes were distinguished in this coding. The first type was the non-terminal nodes or functions where the operators of the algorithm (subtraction, addition, etc.) were housed. They were characterised by always having one or more children. The second type was terminal nodes or leaves of the tree where the fixed values fixed and the variables previously defined were located. These nodes had no children [21].

In a broader application, GP was useful to elaborate mathematical expressions. Its way of encoding allows them to be easily represented, so it is widely used in engineering fields. Useful results were obtained, and some expressions were achieved, which were better than the existing ones [21].

A database is required to use GP. In this case, the database was based on the results from the rheological and empirical tests conducted with the designed mixtures. After obtaining the dataset, it was divided into two subsets: one for training, and one for testing.

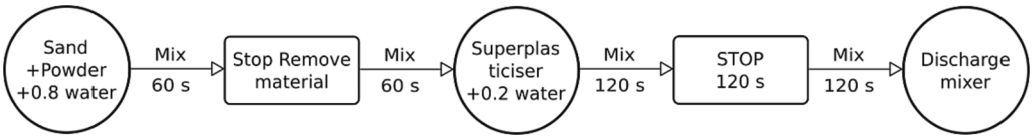

Fig. 3. Mortar mixing procedure.

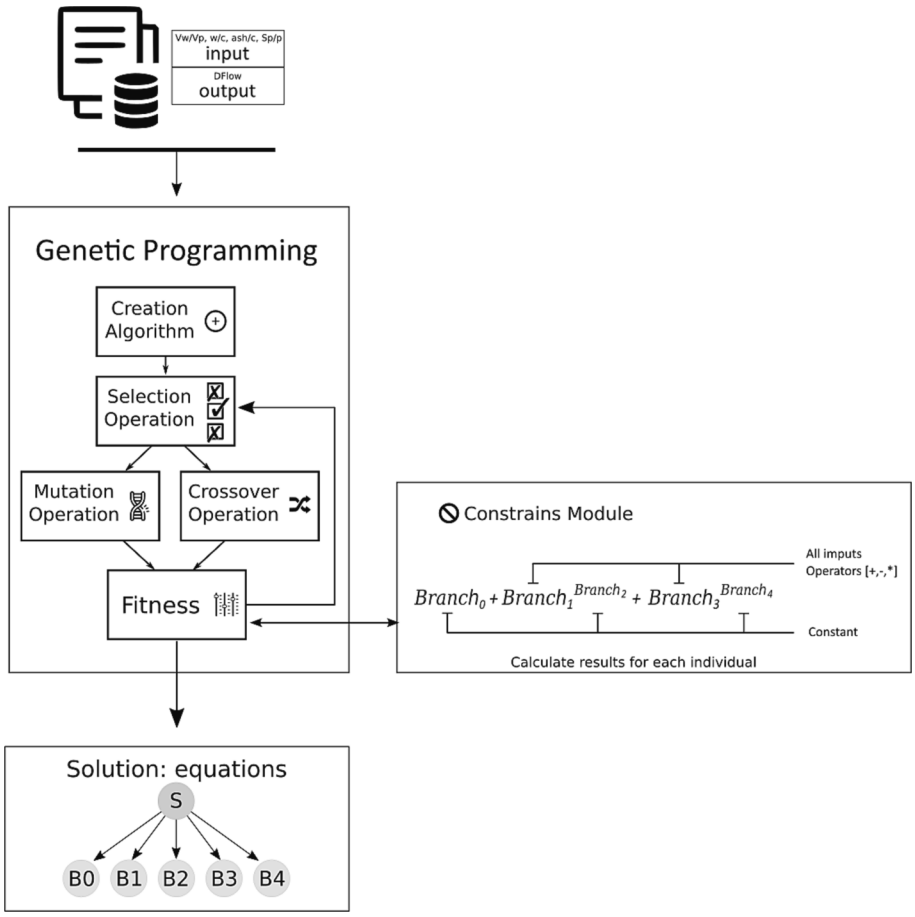

Fig. 4. Algorithm diagram.

4.1. GP application

Table 4 shows the default parameters used in the runs of the algorithm implementation. These parameters were chosen because they gave the best results in the initial tests. The input data to the algorithm were not normalised, unlike other techniques such as ANN, to make the resulting equations applicable.

Table 4
GP in mortar.

	Dflow	Tfunnel
Configuration parameters	Default values	Default values
Population size	1000	1000
Crossover rate	80%	80%
Non-terminal selection rate	90%	90%
Mutation probability	20%	20%
Algorithms	Selection: Tournament Creation: intermediate Mutation: subtree	Selection: Tournament Creation: intermediate Mutation: subtree
Parsimony	0	0.001
Elitist	1	1
Initial tree height	6	6
Maximum tree height	9	9
Maximum mutation tree height	6	6
Terminal nodes	V_W/V_P w/c Sp/P ash/c	V_W/V_P w/c Sp/P ash/c
Non-terminal nodes	+, -, *,	+, -, *, %,

Firstly, GP was used without constraints [36]. After analysing the equations from this initial phase, constraints were defined for the properties that required them according to the analysis of the statistical parameters of the equation obtained. To guide the search process of the GP algorithm, it was necessary to define a set of core equations in which the GP algorithm was allowed to modify only at specific points, which were called branches. Different constraints were established on each branch.

To obtain the equation that predicts the values of mini cone spread diameter and time to pass the mini funnel for mortars, a first attempt was made under free programming. After analysing the results, one improved equation was found for Tfunnel, but no equation improved the results from the design of experiments (DOE) analysis, so an equation was selected to be used as a guide as follows:

$$Dflow_{PG} = Branch_0 + Branch_1^{\,Branch_2} + Branch_3^{\,Branch_4} \quad (1)$$

The following restrictions were set for each branch: $Branch_0$, $Branch_2$ and $Branch_4$ to be a constant, and $Branch_2$ and $Branch_4$ to be a positive

Table 5
Performance indices.

$MSE = \frac{1}{n}\sum_{i=1}^{n}(x_i - y_i)^2$	Eq. 2
$MAE = \frac{1}{n}\sum_{i=1}^{n} abs(x_i - y_i)$	Eq. 3
$COV = \frac{\sqrt{\frac{\sum_{i=1}^{n}(x_i - \bar{x})^2}{n}}}{\frac{\sum_{i=1}^{n}(x_i)}{n}} \bullet 100$	Eq. 4
$R^2 = \left(\frac{\sum_{i=1}^{n}(x_i - \bar{x}) \bullet (y_i - \bar{y})}{\sqrt{\sum_{i=1}^{n}(x_i - \bar{x})^2 (y_i - \bar{y})^2}}\right)^2$	Eq. 5

constant with 2 decimal places as maximum. Finally, $Branch_1$ and $Branch_3$ could contain any input variable and the operators +, − and * up to 5 times for each branch.

Final models were performed by measuring four statistical indicators, i.e. the square of the Pearson product-moment correlation coefficient (R2) Eq. (5), the mean square error (MSE) Eq. (2), the coefficient of variation (COV) Eq. (4), and the mean absolute error (MAE) Eq. (3). These indices allowed the best equations to be determined to predict the measured property accurately. The mathematical equations for the mentioned statistical indicators are presented in Table 5. Moreover, the ratio V_{exp}/V_{pred} that represented the relationship between the value obtained in the experimental test and the value predicted with the adjusted equation was calculated to estimate the accuracy of the models.

4.2. Mortar datasets

The data used as mortar database were the result of the previous experimental campaign. Data, which are included in Table 6, were divided into two sets to conduct this study. A total of 27 mixtures were used for training, and the remaining 6 for testing. It can be observed that Ci mixtures with the same input variables provided different output results because of the intrinsic error related to the test itself.

5. Mortar analysis

The two measured properties of the mortars, Dflow and Tfunnel, were analysed by using the GP technique. The parameters used as input variables were V_W/V_P, w/c, Sp/p, and ash/c.

5.1. Dflow and Tfunnel results

The adjustment developed using GP to predict Dflow and Tfunnel provided Eq. (6) and Eq. (7), respectively. These equations were obtained by applying the GP techniques as explained in Section 4.1.

Table 6
Mortar dataset.

	Code	Dflow (mm)	T funnel (s)
Training	C1	318.75	17.5
	C2	315.75	23.6
	C3	326.00	20.1
	C4	313.00	21.2
	F1	219.75	43.2
	F2	343.25	12.7
	F3	207.50	61.8
	F4	327.75	16.5
	F5	258.50	33.5
	F6	336.00	12.9
	F7	260.50	39.2
	F8	339.75	13.1
	F9	231.50	45.8
	F10	333.50	12.8
	F11	226.50	51.2
	F12	333.50	14.2
	F13	281.75	31.8
	F14	329.25	14.2
	F15	278.50	37.0
	F16	332.25	15.3
	CC2	364.00	9.2
	CC3	310.00	23.1
	CC4	301.00	22.5
	CC5	305.50	19.2
	CC6	332.50	18.8
	CC7	319.50	23.7
	CC8	330.75	18.3
Test	C	308.50	21.3
	C	325.50	17.1
	C	317.25	19.0
	CC1	315.75	20.3
	CC7	290.25	24.9
	CC8	324.16	18.0

$$Tfunnel_{PG} = \frac{38*\frac{w}{c}}{336*\frac{Sp}{p} + \left(\left(\frac{Vw}{Vp} - 1\right)\right)\left(\frac{w}{c} + 23\right)} + \frac{558*SpP + \left(\frac{4}{\frac{ash}{c}}\right)}{\left(\left(\frac{Vw}{Vp} - 1\right)\right)\left(\frac{Vw}{Vp} + 16\right) + 6} + \frac{1}{4*\left(\frac{ash}{c}\right)^2*(6400*\frac{Sp}{p} - 250*\frac{w}{c})} \quad (7)$$

Both equations were analysed by comparing their accuracy with the accuracy of the equations obtained in a previous study (Eqs. (8) and (9)) [29].

$$Dflow_{PG} = 18.7893 + \left(0.5*\left(\left(3 - \left(\left(\left(\left(\frac{Vw}{Vp}*0.1\right)*\frac{Vw}{Vp}\right)*\left(6 + \left(2*\frac{w}{C}\right)\right)\right)*\left(\left(6 + \left(2*\frac{w}{c}\right)\right)*0.5\right)\right)\right) + \left(0.1 + \frac{Vw}{Vp}\right)\right)\right)^9 + \left(-11*\frac{Sp}{p} + 5*\frac{Vw}{Vp} + \frac{w}{c} + \left(\frac{w}{c} + \frac{9}{100}\right)*\left(\left(\frac{Vw}{Vp}\right)^2*\frac{ash}{c} - 6*\frac{ash}{c}*\frac{w}{c}\right)*\left(72*\frac{Sp}{p} + 90*\frac{Vw}{Vp} - 3*\frac{w}{c} - 86\right)*\left(72*\frac{Sp}{p} + \frac{\left(\frac{ash}{c}\right)^2}{10} + \frac{\frac{ash}{c}}{20} - \frac{\frac{w}{c}}{2} - \frac{17}{20}\right) - \frac{6003}{1000}\right)^9 \quad (6)$$

Table 7
Statistical indicators.

	Dflow $_{DOE}$	Dflow $_{PG}$	Tfunnel $_{DOE}$	Tfunnel $_{PG}$
COV	5.9428	5.5172	14.6961	8.4104
V_{exp}/V_{pred}	0.9883	0.9910	1.0327	1.0004
Max (exp/pred)	1.0661	1.0554	1.4963	1.2270
Min (exp/pred)	0.6978	0.7345	0.7705	0.8358
R^2	0.9447	0.9534	0.8367	0.9784
ECM	178	153	25	3
EM	8.89	9.07	3.13	1.24
Demerit	–	133	–	123

$$Dflow_{DOE} = -12245.407 + 18197.271 \bullet \frac{Vw}{Vp} + 2036.667 \bullet \frac{w}{c} + 434447.917 \frac{Sp}{p} + 3962.708 \bullet \frac{ash}{c} - 486875.000 \bullet \frac{Vw}{Vp} \bullet \frac{Sp}{p} - 4512.500 \bullet \frac{Vw}{Vp} \bullet \frac{ash}{c} - 5199.375 \bullet \left(\frac{Vw}{Vp}\right)^2 - 2074.375 \bullet \left(\frac{w}{c}\right)^2 \quad (8)$$

$$\frac{1}{Tfunnel_{DOE}} = -0.375 + 0.499 \bullet \frac{Vw}{Vp} \quad (9)$$

The two equations predicted by Dflow (the one obtained with GP and the one from the literature) presented a "similar appearance", and were the sum of variables operators with linear and quadratic interactions of independent variables in both equations. Furthermore, all the independent variables were used in both equations, thus suggesting that they influenced the flow behaviour of the mixtures analysed. The variable V_W/V_P was one of the most present variables in the equation, as well as the w/c ratio.

Considering the previous analysis and the values of the statistical indicators (Table 7), the equation obtained with the GP technique showed better statistical indices. In addition, ECM was reduced by 14%. That equation was slightly more complicated, but accuracy was improved.

As for Tfunnel, the difference between the two equations was significant. In the equation obtained through GP, all the independent variables were involved in the equation with linear and quadratic interactions of independent variables. However, the equation obtained from the literature only depended on the variable V_W/V_P. Although it was expected that this variable was fundamental in the behaviour, it was not the only one that governed the response of the mixtures analysed. According to the statistical indicators (Table 7), it can be concluded that

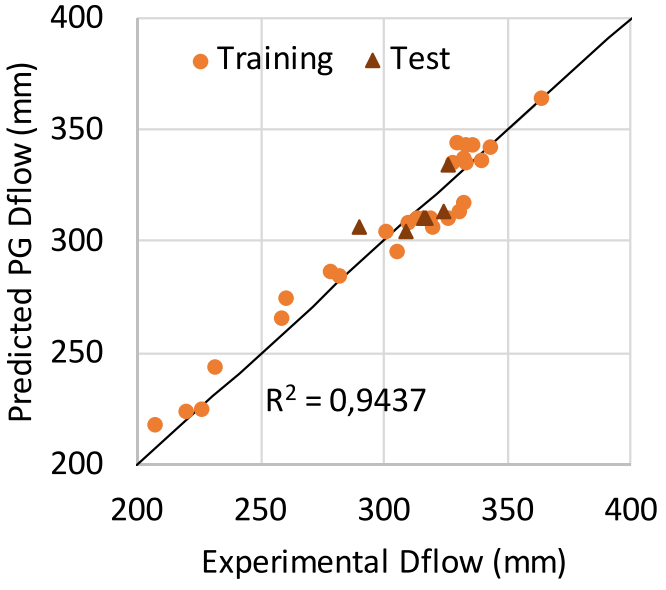

Fig. 5. Experimental vs predicted values (Dflow).

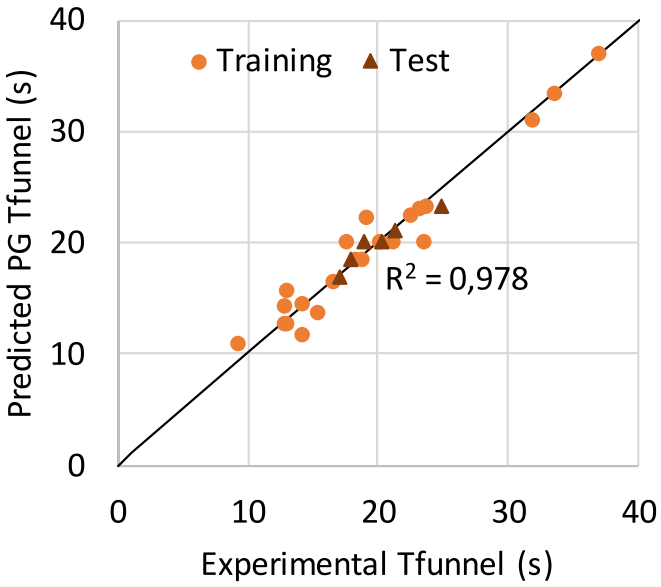

Fig. 6. Experimental vs predicted values (Tfunnel).

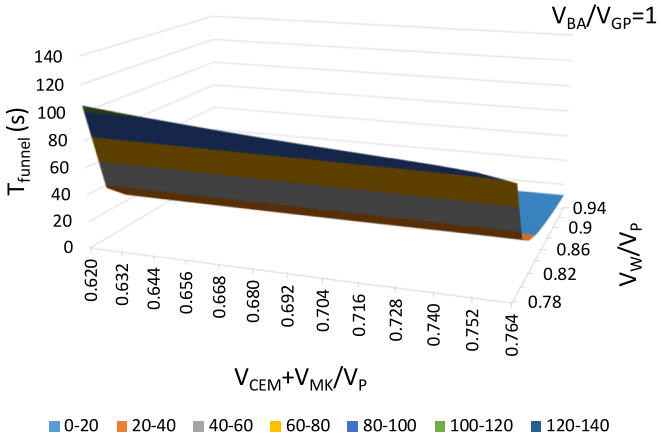

Fig. 7. $(V_C + V_{MK})/V_P$ influence on Tfunnel.

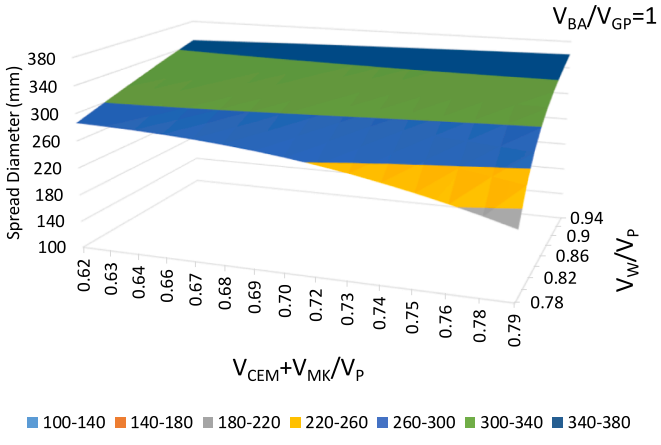

Fig. 8. $(V_C + V_{MK})/V_P$ influence on Dflow.

the equation obtained through the PG greatly improved statistical indexes, thus reducing ECM by 88% and reaching R2 values greater than 0.95.

The relationship between the values obtained experimentally and those determined using the adjusted equation is shown in Fig. 5 and Fig. 6. Both equations showed R2 greater than 0.94.

5.2. Parametric analysis

One of the main advantages of GP is that, after obtaining an equation, it can be used to analyse the influence of different parameters on the measured property throughout the parametric analysis.

Fig. 7 and Fig. 8 were drawn to analyse the influence of the (V_{CEM} + V_{MK})/V_P on Tfunnel and the spread diameter by keeping the V_{BA}/V_{GP} fixed at 1. Therefore, when active powders increased, unreactive powders decreased, maintaining the same proportion with the amount of granite equal to the amount of ash.

The quantity of active powders was a significant parameter that influenced concrete rheology as it controlled water demand. When the quantity of water was high, the increase of (V_{CEM} + V_{MK})/V_P hardly affected the spread diameter or Tfunnel. On the contrary, when the quantity of water was low, the spread diameter was reduced (around 30%), as well as Tfunnel (around 25%).

The spread diameter was a parameter highly affected by the water demand of active powders. When the quantity of water was low, the increase of the active powder increased water demand and decreased the spread diameter.

On the other hand, although Tfunnel was influenced by water demand, it was also affected by the interaction among particles, with the shape and texture of the fine particles being significant properties after analysing this parameter. The increase in active powders not just affected water demand, but also the quantity of BA and GP introduced in the mix. These sup. lementary materials seemed to affect Tfunnel so negatively that the negative effect of increasing the water demand was being counteracted by the positive effect of the shape of the particles of the cement and MK when compared to the shape of the particles of BA or GP. When the interaction among particles was the predominant effect (low water content), then increasing powder materials with better particle geometries reduced the Tfunnel time. The following analysis showed these results and showed the two powder materials (BA or GP) that were affecting Tfunnel so negatively.

Fig. 7 and Fig. 8 also show that an increase in water content increased the spread diameter and decreased Tfunnel. The effect was significant (around 85% in both parameters) when the content of the active powders was high ((V_{CEM} + V_{MK})/V_P of 0.79). When their content was low ((V_{CEM} + V_{MK})/V_P of 0.62), the effect was significant in Tfunnel (around 90%), while in the spread diameter was moderated (around

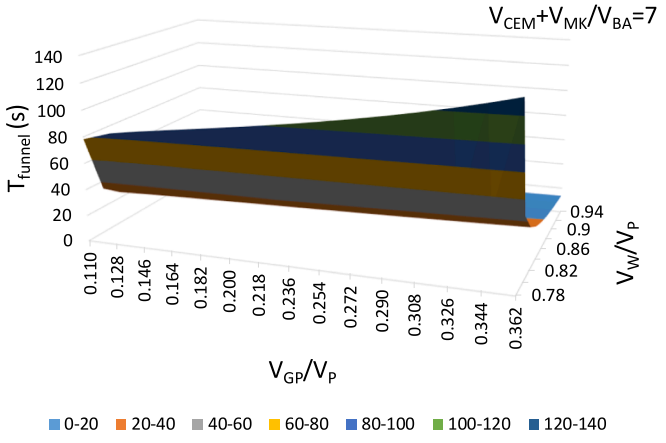

Fig. 9. V_{GP}/V_P influence on Tfunnel.

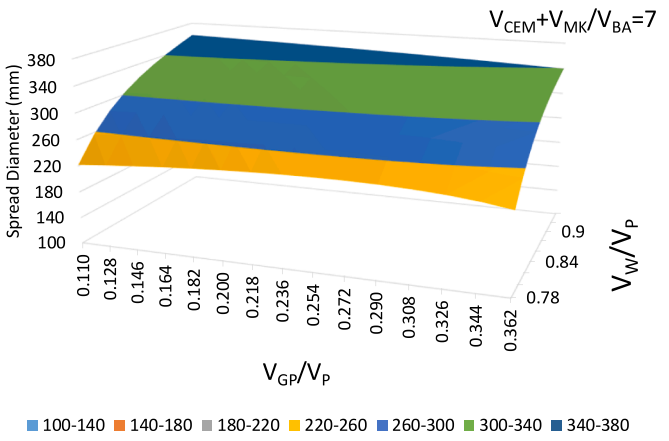

Fig. 10. V_{GP}/V_P influence on Dflow.

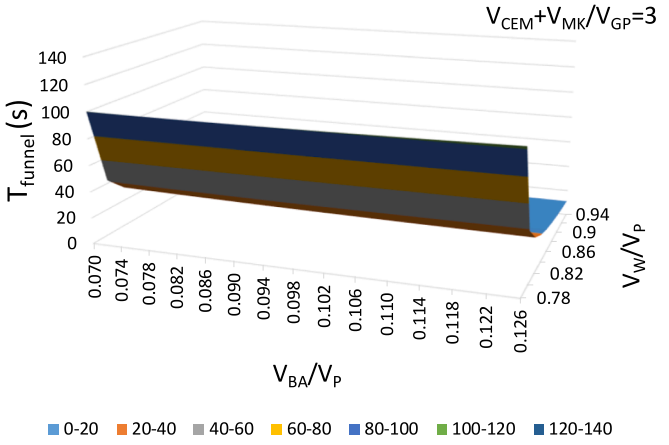

Fig. 11. V_{BA}/V_P influence on Tfunnel.

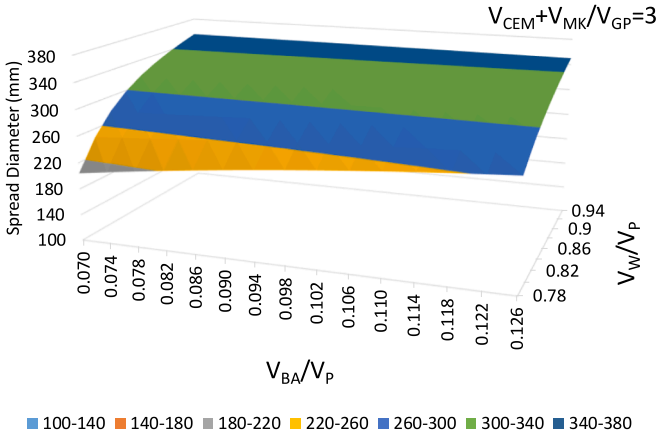

Fig. 12. V_{BA}/V_P influence on Dflow.

22%).

Fig. 9 and Fig. 10 show changes in Tfunnel and Dflow when GP content was modified, while the relationship between active powders and BA was constant. The spread diameter was slightly affected, decreasing its value when the amount of granite power increased. As aforementioned, increasing the GP content decreased cement and MK volume, so water demand was reduced. However, GP included particles with a high irregular shape, and its fineness was higher than the finesses of MK cement. Both effects (reduction in water demand and worse

particle geometry) counteracted, and finally the spread diameter was slightly reduced.

Tfunnel, however, was highly affected by GP content. When water content was low, Tfunnel increased by 70% due to the increase in GP content. When water content was high, this percentage was reduced to 20%, thus indicating that, although there was plenty of water, the negative effect of including GP in Tfunnel values was significant.

Finally, as in the previous analysis, an increase in water content increased spread and decreased Tfunnel. The effect was similar regardless of GP content, and it was more significant (around 87%) in Tfunnel than in the spread diameter (around 51%).

Fig. 11 and Fig. 12 show the effect of BA content in both the spread diameter and Tfunnel when the relationship was constant between active powders and GP.

When the quantity of water was high, the spread diameter was hardly affected and remained around 350 mm regardless of the quantity of BA. When water content was reduced and BA was increased, the spread diameter increased. Likewise, increasing BA reduced the amount of cement and MK, so water demand was reduced. The particles of BA seemed to not damage the spread diameter so much as the particles of GP, so the effect of reducing water demand prevailed, thus increasing the spread diameter when the BA increased.

The same effect was seen by analysing Tfunnel. This parameter decreased when the BA increased. If the quantity of water was low, the reduction was low (8%), and when water content was high, Tfunnel was reduced by 19%. The BA is a filler with a low fineness (its particle size distribution, included in Fig. 2, showed that this material was coarser than cement, MK or GP).

The increase in water content increased the spread diameter and decreased Tfunnel. The effect on Tfunnel was similar regardless of BA content. A percentage of around 87% of decrease in Tfunnel was measured when water content increased from a V_W/V_P of 0.78 to 0.94. This change in water increased the spread diameter by 73% when BA content was low (V_{BA}/V_P of 0.070) and by 33% when BA content was high (V_{BA}/V_P of 0.126). When BA content was high, water demand by the active powder was lower as its volume was also lower, so increasing water hardly affected.

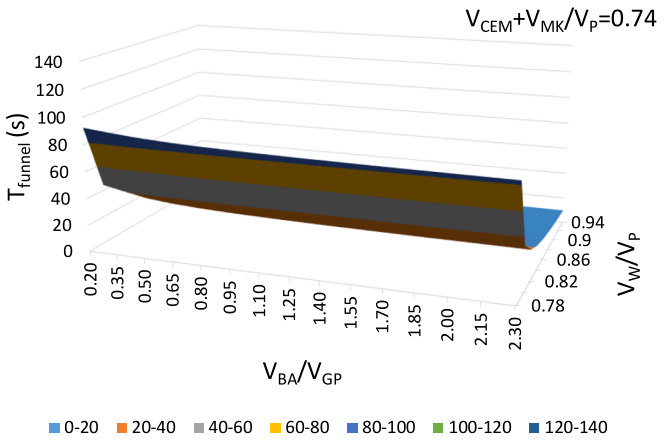

Fig. 13. V_{BA}/V_P influence on Tfunnel.

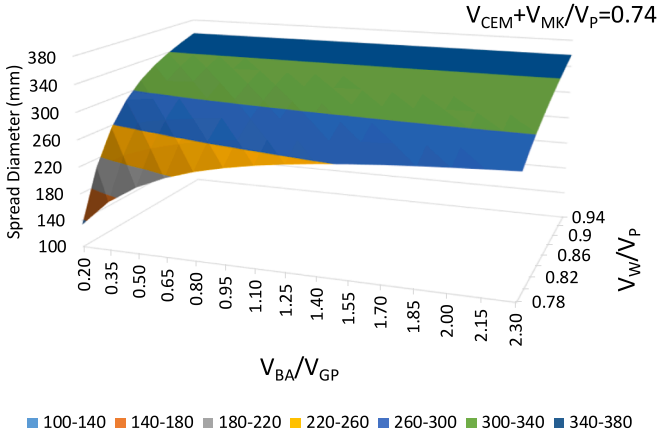

Fig. 14. $V_{BA}/V_P/V_P$ influence on Dflow.

To better analyse the effect of GP in comparison with the effect of BA on Tfunnel and the spread diameter, Fig. 13 and Fig. 14 where drawn. The quantity of active powder was constant ($V_{CEM} + V_{MK}/V_p$) at 0.74, therefore the amount of GP plus BA was also constant ($V_{BA} + V_{GP}/V_P =$ 0.244). However, the relationship between them (V_{BA}/V_{GP}) varied from 0.2 to 2.3.

Both parameters were positively affected by the increase in the BA (thus decreasing GP content): Tfunnel decreased and Dflow increased. As for the effect of increasing BA, when the amount of water was low, Tfunnel was reduced to 9.5%. In this case, this parameter was very high (around 85 s), and it was not affected by only changing the type of powder materials (the relationship V_{BA}/V_{GP}). When water content was high, Tfunnel was reduced by 86%, and in this case increasing the amount of BA by reducing the amount of GP widely affected Tfunnel time (this time was reduced to 44% when V_W/V_P was 0.94 by increasing V_{BA}/V_{GP} from 0.2 to 2.3).

Spread presented great diameter values (around 357 mm) when water content was high. It was difficult to increase more these values when only V_{BA}/V_{GP} was being increased. For this reason, the spread diameter hardly changed by the ratio V_{BA}/V_{GP} when water content was high. On the contrary, when water content was low, the spread diameter significantly improved (from 133 mm to 273 mm) when the V_{BA}/V_{GP} changed from 0.20 to 2.30.

6. Conclusions

This study analysed the possibilities offered by genetic programming to predict the fresh state behaviour of quaternary mortar mixtures. Models obtained were compared with those developed throughout analysis of variance. After comparing both techniques, it was concluded that genetic programming provides better accuracy, according to the statistical parameters selected as performance indicators.

The equations adjusted with genetic programming were used to conduct a parametric analysis of how the different powder materials affected the fresh behaviour of mortar mixes. The following conclusions were drawn:

The influence of metakaolin and cement ($V_{CEM} + V_{MK}$)/V_P on both Tfunnel and the spread diameter was studied, with V_{BA}/V_{GP} being constant. When the quantity of water was high, increasing the cement and metakaolin hardly affected the spread diameter or Tfunnel. On the contrary, when the quantity of water was low, that increase reduced the spread diameter and, unexpectedly, reduced Tfunnel.

When granite powder content was modified and the relationship between active powders and biomass ash was constant, the spread diameter was slightly affected, decreasing its value when the amount of granite power increased. However, Tfunnel widely increased.

The effect of biomass ash content on both the spread diameter and Tfunnel was analysed by keeping the relationship between active powders and granite powder constant. When the biomass ash increased, the spread diameter increased and Tfunnel decreased.

To better analyse the effect of granite powder in comparison with the effect of biomass ash, the quantity of active powders was constant, varying the ratio VBA/VGP. Both parameters, Tfunnel time and spread diameter, were positively affected by the increase in the biomass ash, thus reducing granite powder content: Tfunnel decreased and Dflow increased. Granite powder is a material with a high fineness and their particles are rough and irregular, so its effect on fresh state is negative, especially when the interaction among particles is the predominant

phenomenon (mixes with low water to binder ratio).

Finally, genetic programming and design of experiments are powerful tools that can be used to analyse the influence of multiple parameters in any concrete or mortar property, and their use is recommended in adjusted models that can be employed by the stakeholders to predict these properties.

Declaration of Competing Interest

The authors declare that they have no known competing financial interests or personal relationships that could have appeared to influence the work reported in this paper.

Data availability

Data will be made available on request.

Acknowledgements

This study is part of two projects entitled: "Design of sustainable concrete for 3D printing based on rheology and on the control of very early properties (Eco3DConcrete)- PID2020-115433RB-I00" and "Design of concrete precast elements incorporating sustainable strategies for self-healing to increase their service life (PREHEALING)-PDC2021-121660-I00" funded by MINECO

References

[1] M.I. Shah, M.F. Javed, F. Aslam, H. Alabduljabbar, Machine learning modeling integrating experimental analysis for predicting the properties of sugarcane bagasse ash concrete, Construction and Building Materials 314 (2022) 125634.
[2] H. Li, M. Liebscher, J. Yang, M. Davoodabadi, L. Li, Y. Du, B. Yang, S. Hempel, V. Mechtcherine, Electrochemical oxidation of recycled carbon fibers for an improved interaction toward alkali-activated composites, Journal of Cleaner Production 368 (2022), 133093, https://doi.org/10.1016/J.JCLEPRO.2022.133093.
[3] H. Li, L. Wang, Y. Zhang, J. Yang, D.C.W. Tsang, V. Mechtcherine, Biochar for sustainable construction industry, Curr. Dev. Biotechnol. Bioeng. Biochar Towar. Sustain. Environ. (2023) 63–95. https://doi.org/10.1016/B978-0-323-91873-2.00015-7.
[4] K. Samimi, S. Kamali-Bernard, A. Akbar Maghsoudi, M. Maghsoudi, H. Siad, Influence of pumice and zeolite on compressive strength, transport properties and resistance to chloride penetration of high strength self-compacting concretes, Construction and Building Materials 151 (2017) 292–311, https://doi.org/10.1016/j.conbuildmat.2017.06.071.
[5] R. Saleh Ahari, T. Kemal Erdem, K. Ramyar, Effect of various supplementary cementitious materials on rheological properties of self-consolidating concrete, Construction and Building Materials 75 (2015) 89–98, https://doi.org/10.1016/j.conbuildmat.2014.11.014.
[6] R.S. Ahari, T.K. Erdem, K. Ramyar, Thixotropy and structural breakdown properties of self consolidating concrete containing various supplementary cementitious materials, Cement and Concrete Composites 59 (2015) 26–37, https://doi.org/10.1016/j.cemconcomp.2015.03.009.
[7] M. Nazeer, K. Kapoor, S.P. Singh, Strength, durability and microstructural investigations on pervious concrete made with fly ash and silica fume as supplementary cementitious materials, J. Build. Eng. 69 (2023), 106275, https://doi.org/10.1016/J.JOBE.2023.106275.
[8] C.E. Tino Balestra, L.R. Garcez, L. Couto da Silva, M.T. Veit, E. Jubanski, A. Y. Nakano, M.H. Pietrobelli, R. Schneider, M.A. Ramirez Gil, Contribution to low-carbon cement studies: Effects of silica fume, fly ash, sugarcane bagasse ash and acai stone ash incorporation in quaternary blended limestone-calcined clay cement concretes, Environ. Dev. 45 (2023), 100792, https://doi.org/10.1016/J.ENVDEV.2022.100792.
[9] C. Dong, Q. Zhang, C. Chen, T. Jiang, Z. Guo, Y. Liu, S. Lin, Fresh and hardened properties of recycled plastic fiber reinforced self-compacting concrete made with recycled concrete aggregate and fly ash, slag, silica fume, J. Build. Eng. 62 (2022), 105384, https://doi.org/10.1016/J.JOBE.2022.105384.
[10] G. Rojo-López, B. González-Fonteboa, F. Martínez-Abella, I. González-Taboada, Rheology, durability, and mechanical performance of sustainable self-compacting concrete with metakaolin and limestone filler, Case Studies in Construction Materials 17 (2022) e01143.
[11] A. Arun Solomon, M. Selvarathi, N. Anand, Influence of supplementary cementitious materials on stress-strain behaviour and toughness characteristics of concrete subjected to higher temperature exposure, materials today: Proceedings (2023).
[12] H.H.Y. Al-Radi, S. Dejian, H.K. Sultan, Performance of fiber self compacting concrete at high temperatures, Civ. Eng. J. 7 (2021) 2083–2098, https://doi.org/10.28991/CEJ-2021-03091779.
[13] M. Gesoğlu, E. Güneyisi, M.E. Kocabağ, V. Bayram, K. Mermerdaş, Fresh and hardened characteristics of self compacting concretes made with combined use of marble powder, limestone filler, and fly ash, Construction and Building Materials 37 (2012) 160–170, https://doi.org/10.1016/j.conbuildmat.2012.07.092.
[14] K. Sobolev, M. Kozhukhova, K. Sideris, E. Menéndez, M. Santhanam, Alternative supplementary cementitious materials, RILEM State-of-the-Art Reports. 25 (2018) 233–282, https://doi.org/10.1007/978-3-319-70606-1_7.
[15] A.A. Jhatial, I. Nováková, E. Gjerløw, A Review on Emerging Cementitious Materials, Reactivity Evaluation and Treatment Methods, Buildings 13 (2) (2023) 526.
[16] M. Mohtasham Moein, A. Saradar, K. Rahmati, S.H. Ghasemzadeh Mousavinejad, J. Bristow, V. Aramali, M. Karakouzian, Predictive models for concrete properties using machine learning and deep learning approaches: A review, J. Build. Eng. 63 (2023), 105444, https://doi.org/10.1016/J.JOBE.2022.105444.
[17] J.-S. Chou, C.-F. Tsai, A.-D. Pham, Y.-H. Lu, Machine learning in concrete strength simulations: Multi-nation data analytics, Construction and Building Materials 73 (2014) 771–780, https://doi.org/10.1016/j.conbuildmat.2014.09.054.
[18] F. Farooq, W. Ahmed, A. Akbar, F. Aslam, R. Alyousef, Predictive modeling for sustainable high-performance concrete from industrial wastes: A comparison and optimization of models using ensemble learners, Journal of Cleaner Production 292 (2021), 126032, https://doi.org/10.1016/j.jclepro.2021.126032.
[19] G.R. Abdollahzadeh, E. Jahani, Z. Kashir, Genetic Programming Based Formulation to Predict Compressive Strength of High Strength Concrete, Civ. Eng. Infrastructures J. 50 (2017) 207–219, https://doi.org/10.7508/ceij.2017.02.001.
[20] G. Ma, Y. Wang, H.-J. Hwang, Genetic programming-based backbone curve model of reinforced concrete walls, Genetic programming-based backbone curve model of reinforced concrete walls 283 (2023) 115824.
[21] J.L. Pérez, A. Cladera, J.R. Rabuñal, F. Martínez-Abella, Optimization of existing equations using a new Genetic Programming algorithm: Application to the shear strength of reinforced concrete beams, Advances in Engineering Software 50 (2012) 82–96, https://doi.org/10.1016/j.advengsoft.2012.02.008.
[22] I. González-Taboada, B. González-Fonteboa, F. Martínez-Abella, J.L. Pérez-Ordóñez, Prediction of the mechanical properties of structural recycled concrete using multivariable regression and genetic programming, Construction and Building Materials 106 (2016) 480–499, https://doi.org/10.1016/j.conbuildmat.2015.12.136.
[23] S. Nazar, J. Yang, A. Ahmad, S.F.A. Shah, Comparative study of evolutionary artificial intelligence approaches to predict the rheological properties of fresh concrete, Materials Today Communications 32 (2022), 103964, https://doi.org/10.1016/J.MTCOMM.2022.103964.
[24] M. Ben aicha, Y. Al Asri, M. Zaher, A.H. Alaoui, Y. Burtschell, Prediction of rheological behavior of self-compacting concrete by multi-variable regression and artificial neural networks, Powder Technology 401 (2022), 117345, https://doi.org/10.1016/J.POWTEC.2022.117345.
[25] A. Mohammed, S. Rafiq, W. Mahmood, H. Al-Darkazalir, R. Noaman, W. Qadir, K. Ghafor, Artificial Neural Network and NLR techniques to predict the rheological properties and compression strength of cement past modified with nanoclay, Ain Shams Engineering Journal 12 (2021) 1313–1328, https://doi.org/10.1016/J.ASEJ.2020.07.033.
[26] M. Aziminezhad, M. Mahdikhani, M.M. Memarpour, RSM-based modeling and optimization of self-consolidating mortar to predict acceptable ranges of rheological properties, Construction and Building Materials 189 (2018) 1200–1213, https://doi.org/10.1016/J.CONBUILDMAT.2018.09.019.
[27] S. Nazar, J. Yang, M. Faisal Javed, K. Khan, L. Li, Q. feng Liu, An evolutionary machine learning-based model to estimate the rheological parameters of fresh concrete, Structures. 48 (2023) 1670–1683, https://doi.org/10.1016/J.ISTRUC.2023.01.019.
[28] I. Navarrete, I. La Fé-Perdomo, J.A. Ramos-Grez, M. Lopez, Predicting the evolution of static yield stress with time of blended cement paste through a machine learning approach, Construction and Building Materials 371 (2023), 130632, https://doi.org/10.1016/J.CONBUILDMAT.2023.130632.
[29] G. Rojo-López, S. Nunes, B. González-Fonteboa, F. Martínez-Abella, Quaternary blends of portland cement, metakaolin, biomass ash and granite powder for production of self-compacting concrete, Journal of Cleaner Production 266 (2020), 121666, https://doi.org/10.1016/j.jclepro.2020.121666.
[30] M. Pavlíková, L. Zemanová, J. Pokorný, M. Záleská, O. Jankovský, M. Lojka, Z. Pavlík, Influence of Wood-Based Biomass Ash Admixing on the Structural, Mechanical, Hygric, and Thermal Properties of Air Lime Mortars, Materials (Basel). 12 (2019) 2227, https://doi.org/10.3390/ma12142227.

[31] I. Navarrete, Y. Kurama, N. Escalona, M. Lopez, Impact of physical and physicochemical properties of supplementary cementitious materials on structural build-up of cement-based pastes, Cement and Concrete Research 130 (2020), 105994, https://doi.org/10.1016/j.cemconres.2020.105994.
[32] H.H.C. Wong, A.K.H. Kwan, Packing density of cementitious materials: Part 1-measurement using a wet packing method, Mater. Struct. Constr. 41 (2008) 689–701, https://doi.org/10.1617/s11527-007-9274-5.
[33] NF P18-513 – Addition for concrete – Metakaolin – Specifications and conformity criteria, n.d.
[34] AENOR, UNE -EN 196-1. Cement Test Methods. Part 1: Determination of Mechanical Resistances (in Spanish), Madrid, Spain. 2005.
[35] D.C. Montgomery, Design and Analysis of Experiments, Technometrics 48 (2006) 158, https://doi.org/10.1198/tech.2006.s372.
[36] J.R. Koza. Genetic programming : on the programming of computers by means of natural selection. (1992). 819.